DOI: 10.1002/asia.200700318

Generalized Nonaqueous Sol–Gel Synthesis of Different Transition-Metal Niobate Nanocrystals and Analysis of the Growth Mechanism

Lizhi Zhang,*[b, c] Georg Garnweitner,[d] Igor Djerdj,[a] Markus Antonietti,[b] and Markus Niederberger*[a]

Abstract: A general nonaqueous route for the synthesis of phase-pure transition-metal niobate ($InNbO_4$, $MnNb_2O_6$, and $YNbO_4$) nanocrystals was developed based on the one-pot solvothermal reaction of niobium chloride and the corresponding transition-metal acetylacetonates in benzyl alcohol at 200 °C. All samples were carefully characterized by XRD, TEM, HRTEM, and energy-dispersive X-ray (EDX) analysis. The crystallization mechanism of these niobate nanocrystals points to a two-step pathway. First, metal hydroxide crystals and amorphous niobium oxide are formed. Second, metal niobate nanocrystals are generated from the intermediates by a dissolution–recrystallization mechanism. The reaction mechanisms, that is, the processes responsible for the oxygen supply for oxide formation, were found to be rather complex and involve niobium-mediated ether elimination as the main pathway, accompanied by solvolysis of the acetylacetonate ligands and benzylation reactions.

Keywords: crystal growth · nanoparticles · niobium · sol–gel processes · ternary metal oxides

Introduction

Metal oxides represent one of the most diverse classes of materials with important structure-related properties. Many metal oxides have properties of superconductivity, ferroelectricity, magnetism, catalysis, gas-sensing capability, and so on.[1] Some of these properties can be enhanced by decreasing the size of metal oxides to the nanometer scale. Thus, great effort has been made to synthesize different nanostructured metal oxides. These efforts mainly focused on the synthesis and the study of the structure-related properties of binary metal oxide nanostructures. In comparison with binary metal oxides, relatively little work has been performed on the fabrication of ternary metal oxide nanocrystals,[2–5] thus hindering further experimental investigations into the size-dependent properties of these technologically important materials.

Ternary metal oxides are traditionally synthesized by high-temperature solid-state ceramic reactions that often require several days of thermal treatment at temperatures higher than 1000 °C. This is because solid–solid diffusion is the rate-limiting step in their formation.[6,7] It is therefore difficult to control the morphology or the kinetics of phase formation during high-temperature ceramic synthesis. For instance, for the preparation of $MnNb_2O_6$, ground MnO_2 and Nb_2O_5 were heated slowly to 930 °C, held at that temperature for 22 h, then reground and fired at 1200 °C for

[a] Dr. I. Djerdj, Prof. Dr. M. Niederberger
Department of Materials
Swiss Federal Institute of Technology (ETH) Zürich
Wolfgang-Pauli-Str. 10
CH-8093 Zürich (Switzerland)
Fax: (+41) 44-632-1101
E-mail: markus.niederberger@mat.ethz.ch

[b] Prof. Dr. L. Zhang, Prof. Dr. M. Antonietti
Max Planck Institute of Colloids and Interfaces
Colloid Department, Research Campus Golm
D-14424 Potsdam (Germany)

[c] Prof. Dr. L. Zhang
Key Laboratory of Pesticide and Chemical Biology of the Ministry of Education, College of Chemistry
Central China Normal University
Wuhan 430079 (China)
E-mail: zhanglz@mail.ccnu.edu.cn

[d] Prof. Dr. G. Garnweitner
Institute for Particle Technology
Technical University Braunschweig
Volkmaroder Str. 4
38104 Braunschweig (Germany)

Supporting information for this article is available on the WWW under http://www.chemasianj.org or from the author.

36 h with one intermediate regrinding. Recently, soft (or solution) chemical routes, including sol–gel, microemulsion, hydrothermal, and solvothermal methods, have been successfully utilized to prepare various nanosized metal oxides with good control over their morphology, crystal phase, and size. Unfortunately, the formation of single-phase ternary metal oxides by soft chemical routes is not as successful as that of binary oxides because the reactivities of the different metal oxide precursors are different in solution. One way to diminish the problem is to switch from aqueous to nonaqueous reaction media. This approach was successfully applied to various metal oxide nanoparticles with the spinel structure.[8,9] Ternary metal oxide nanocrystals, mainly from the family of ABO_3-type perovskites,[10–14] were also prepared by our group by using benzyl alcohol as well as ketone-based nonaqueous sol–gel methods. Among the various ternary metal oxides, metal niobates are important owing to their pronounced electrical, optical, ferroelectric, and catalytic properties. We developed a nonaqueous method of synthesizing $LiNbO_3$ by the reaction between niobium(V) ethoxide and lithium metal dissolved in benzyl alcohol at 220 °C.[10] Recently, we prepared the nanocrystalline visible-light photocatalyst $InNbO_4$ by a soft-chemistry route involving the solvothermal reaction of indium acetylacetonate and niobium chloride in benzyl alcohol at 200 °C. We found that the as-synthesized nanopowder exhibited a much higher photocatalytic activity than that obtained with traditional high-temperature ceramic methods under visible light.[15]

We report in this study the synthesis of not only $InNbO_4$, but also $YNbO_4$ and $MnNb_2O_6$ nanocrystals by the solvothermal reaction of niobium chlorides and transition-metal acetylacetonates in benzyl alcohol, thus indicating the generality of this process for producing nanosized metal niobates.

There is growing evidence, especially from studies in the field of biomineralization, that points to the existence of crystallization pathways that go beyond the simple attachment of ions or molecules to a growing nucleus.[16] The crystallization of nanomaterials also seems to be more complex than originally anticipated. The exact growth mechanisms involved with most of the synthetic methods used for creating ternary metal oxide nanostructures are often a matter of speculation.[1] Recently, we reported a surprising and unprecedented crystallization pathway for the formation of indium tin oxide nanoparticles, which did not crystallize in a simple nucleation-and-growth process, but first formed an intermediary phase consisting of aligned nanocrystallites embedded in an organic matrix, followed by the transformation into the bixbyite structure with larger crystallites accompanied by the disappearance of both the organic phase and the superstructure.[17] For the metal niobates synthesized in this study, we found another growth mechanism that reveals the unusual and unpredictable crystallization behavior of ternary metal oxides in benzyl alcohol.

Abstract in Chinese:

利用苯甲醇中氯化铌和对应的过渡金属乙酰丙酮盐在 200 摄氏度下“一锅煮”溶剂热反应，我们发展了一个制备过渡金属铌酸盐($InNbO_4$, $MnNb_2O_6$, 和 $YnbO_4$)纳米晶的通用非水溶胶-凝胶合成路线。通过对所有样品的 XRD, TEM, HRTEM 和 EDX 详细表征，我们发现这些铌酸盐的结晶是经过两步完成。首先是金属氢氧化物晶体和无定形氧化铌的形成，接着这些中间体通过一个溶解-再结晶的机理生成铌酸盐纳米晶。其中的化学反应机理(如氧化物形成的氧供应的过程)相当复杂，主要涉及到铌调控的酯消去途径，同时伴随着乙酰丙酮配体的溶剂分解和苯化反应。

Results and Discussion

Powder X-ray diffraction (XRD) patterns of the as-synthesized metal niobate samples are shown in Figure 1. All diffraction peaks in Figure 1a can be assigned to the monoclinic phase of $InNbO_4$ (space group *P*2/*c* (No. 13), JCPDS file No. 33-619) without any indication of crystalline by-products. The most intense peaks at 24.0, 29.5, and 35.6° are the diffractions from the (011), ($\bar{1}$11) and (111), and (120) planes of monoclinic $InNbO_4$, respectively. All the peaks in Figure 1b and c can be well-indexed to the orthorhombic phase of $MnNb_2O_6$ (space group *Pcan* (No. 60), JCPDS file No. 33-899) and the monoclinic phase of $YNbO_4$ (space group *I*2 (No. 5), JCPDS file No. 23-1486), respectively. In Figure 1b, the most prominent peaks at 24.1, 29.8, and 37.2° are the diffractions from the (130) and (111), (131), and (002) planes of orthorhombic $MnNb_2O_6$, respectively, whereas in Figure 1c, the peaks at 29.5, 34.0, and 48.6° are assigned to the ($\bar{1}$21) and (121), (200), and (240) and (042) planes of monoclinic $YNbO_4$, respectively. The XRD results prove that single-phase metal niobates can be obtained by the solvothermal reaction of niobium chloride with the cor-

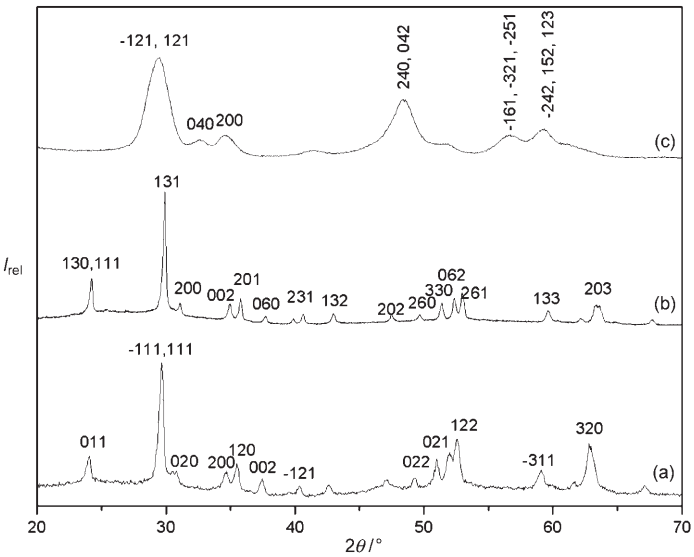

Figure 1. XRD patterns of the as-prepared samples of a) $InNbO_4$, b) $MnNb_2O_6$, and c) $YNbO_4$.

responding transition-metal acetylacetonates in benzyl alcohol.

Representative transmission electron microscopy (TEM) images of the sample of indium niobate are shown in Figure 2. Because of the lack of any stabilizing surfactants, the indium niobate particles are slightly agglomerated (Figure 2a). However, it is easy to estimate the diameters of the particles, which are in the range 10–30 nm. The high crystallinity as well as the single-crystalline nature of the particles is further confirmed by high-resolution TEM (HRTEM) analysis (Figure 2b). Due to the overlapping of several $InNbO_4$ nanoparticles in Figure 2b, the unambiguous determination of the orientation of the zone axis of any of the crystallites was not possible. Therefore, only the resolved lattice fringes, $(0\bar{1}1)$ and $(\bar{2}11)$, of $InNbO_4$ are denoted.

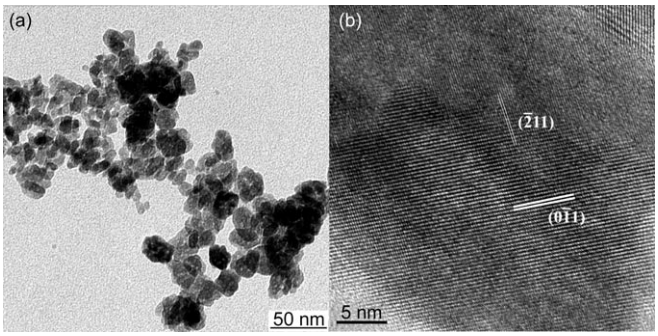

Figure 2. a) TEM and b) HRTEM images of the as-prepared sample of $InNbO_4$. The resolved crystal planes are marked.

Figure 3 shows typical TEM images of the as-prepared $MnNb_2O_6$ sample. The $MnNb_2O_6$ particles are uniform in size with diameters of a few nanometers, which are significantly smaller than those of $InNbO_4$. As with $InNbO_4$, the $MnNb_2O_6$ particles are also slightly agglomerated (Figure 3a). Figure 3b shows one isolated $MnNb_2O_6$ nanoparticle of about 10 nm in diameter. The corresponding power spectrum (fast Fourier transform; Figure 3b, inset) points to the single-crystalline nature of the $MnNb_2O_6$ nanoparticle. Analysis of the distances and angles of the array of discrete spots in the power spectrum reveals that the displayed $MnNb_2O_6$ crystallite is in the $[\bar{3}10]$ zone-axis orientation.

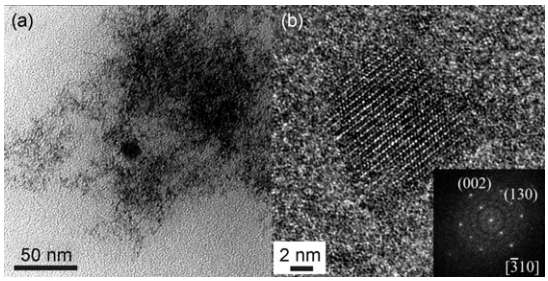

Figure 3. a) TEM and b) HRTEM images of the as-prepared sample of $MnNb_2O_6$. Inset: Corresponding power spectrum with lattice indices.

TEM images of the as-prepared $YNbO_4$ sample are shown in Figure 4. The $YNbO_4$ particles are more agglomerated than those of $InNbO_4$ and $MnNb_2O_6$. The diameters are in the range 10–20 nm (Figure 4a). The HRTEM image in Figure 4b also confirms that the $YNbO_4$ particles are single-crystalline. The well-resolved (002) lattice planes with a *d* spacing of 2.526 Å are indicated.

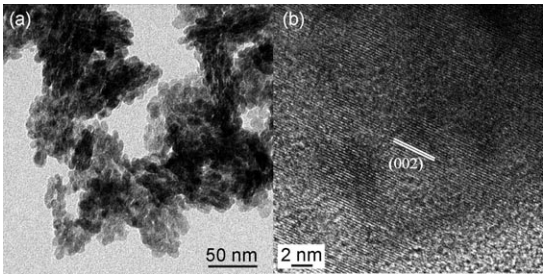

Figure 4. a) TEM and b) HRTEM images of the as-prepared sample of $YNbO_4$.

To understand the growth mechanism of $InNbO_4$ nanoparticles in benzyl alcohol, we studied the intermediates after reaction times of 3 and 6 h. XRD analysis reveals that crystalline $InNbO_4$ was already formed after 3 h (Figure 5a). Besides $InNbO_4$, another set of peaks can be indexed to $In(OH)_3$ (JCPDS file No. 16-0161). Upon extension of the reaction time to 6 h, the intensity of the peaks corresponding to the $InNbO_4$ particles increased. As the initial In/Nb molar ratio is one, and given that $In(OH)_3$ was detected by XRD, an additional niobium-containing compound should also be present in the sample. However, the XRD pattern does not display any reflections of such a compound, which means that the niobium species is amorphous. This is confirmed by TEM and energy-dispersive X-ray (EDX) analysis. Figure 5b shows a TEM image of the sample obtained after 3 h. The EDX spectrum (Figure 5c) reveals that the particles on the left of Figure 5b contain niobium and oxygen, and the HRTEM image (Figure 5d) of these particles shows that they are completely amorphous. On the contrary, the particles on the right of Figure 5b are well-crystalline $InNbO_4$, as confirmed by the EDX spectrum (Figure 5e), which proves the presence of niobium and indium, and by the HRTEM image in Figure 5f. The (011) and (111) lattice planes of $InNbO_4$, which belong to different grains with a random orientation with respect to each other, are indicated in Figure 5f.

On the basis of these results, we propose the following growth mechanism of $InNbO_4$ nanoparticles (Scheme 1). First, indium acetylacetonate and niobium chloride react with benzyl alcohol to produce crystalline $In(OH)_3$ and amorphous niobium oxide. $InNbO_4$ nanoparticles are then generated by the reaction between these species formed in situ. The second process is presumably quite similar to the hydrothermal or sonochemical formation of $SrTiO_3$ (or $BaTiO_3$) from $Sr(OH)_2$ (or $Ba(OH)_2$) and amorphous TiO_2 by a dissolution–crystallization mechanism.[18–22] Amorphous

CHEMISTRY
AN ASIAN JOURNAL

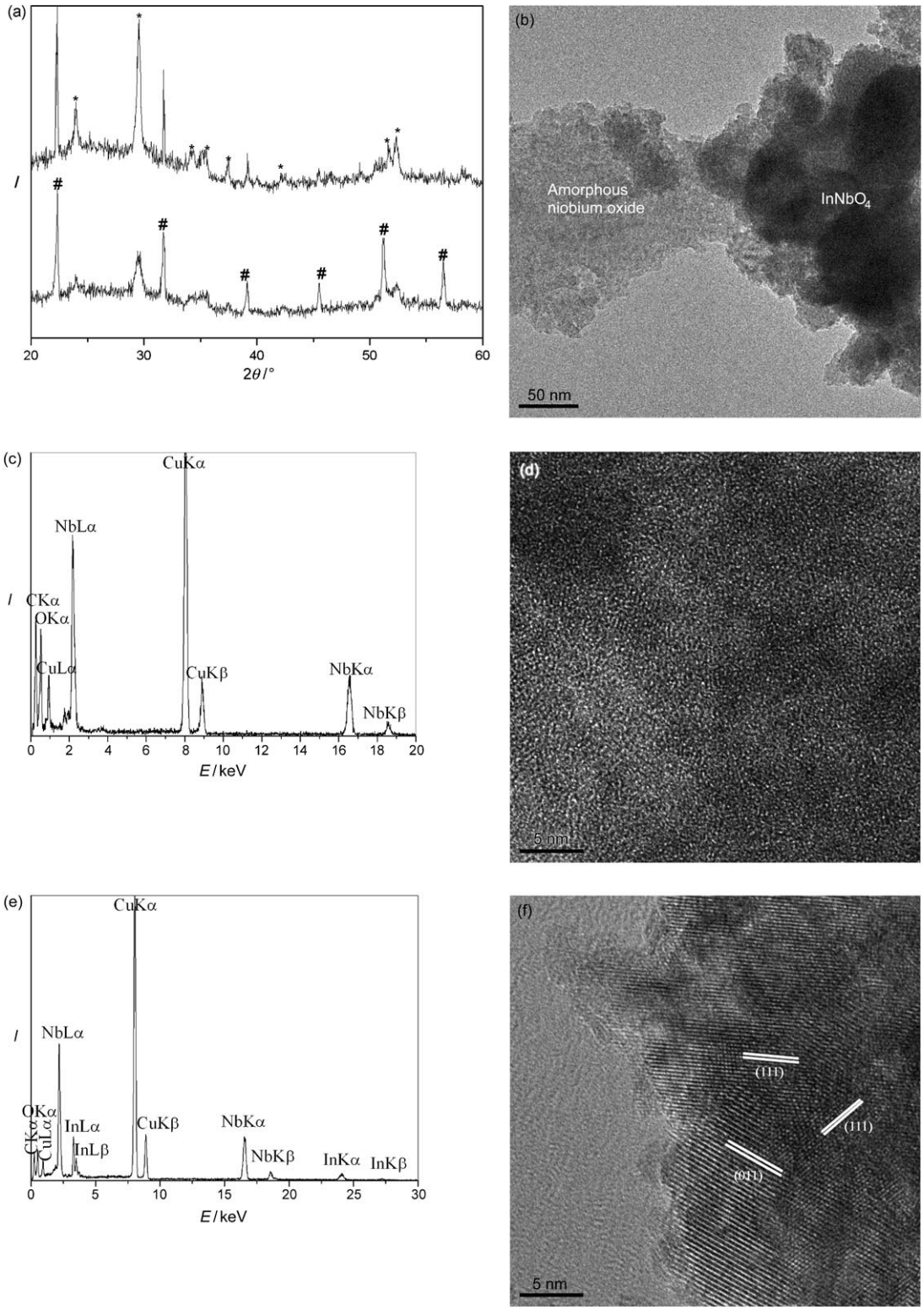

Figure 5. a) XRD patterns of the intermediate samples obtained after 3 h (bottom) and 6 h (top). * = $InNbO_4$, # = $In(OH)_3$. b) TEM image of the sample obtained after 3 h. c) EDX spectrum of the particles on the left in Figure 5b, proving the exclusive presence of Nb and O. d) HRTEM image of the amorphous niobium oxide particles. e) EDX spectrum of the particles on the right in Figure 5b, proving the presence of In, Nb, and O. f) HRTEM image of the particles in e) with lattice planes corresponding to $InNbO_4$.

niobium oxide particles dissolve in benzyl alcohol to form niobium hydroxy species, which instantly react with $In(OH)_3$ at the surface to produce $InNbO_4$ nuclei. Further growth is then promoted by the higher thermodynamic stability of the

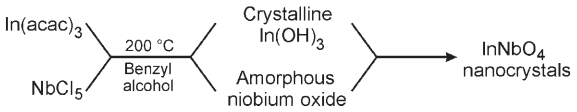

Scheme 1. Formation process of $InNbO_4$ nanocrystals by solvothermal reaction of niobium chloride and indium acetylacetonate ($In(acac)_3$) in benzyl alcohol.

mixed species. Interestingly, we found that the direct solvothermal reaction of $In(OH)_3$ and amorphous niobium oxide at 200 °C did not yield $InNbO_4$. Clearly, some other species produced in situ during the reaction or a different composition of the amorphous intermediate promoted the solubility of the reactants in benzyl alcohol and subsequently supported the formation of the $InNbO_4$ nanocrystals from $In(OH)_3$ and amorphous niobium oxide.

We found that the final reaction solution of these metal niobates consists of two liquid phases, a clear, colorless aqueous phase and a yellow, more viscous organic phase. Both phases were subjected to detailed NMR spectroscopic and GC–MS analyses (see Supporting Information) to identify the individual components and to elucidate the mechanism of the chemical reaction by retroanalysis. The aqueous phase, which is only about one tenth of the total liquid volume, was indeed found to contain water as the main component, as well as some benzyl alcohol, benzyl acetate, and acetone. The organic phase, on the other hand, was found to be very complex and quite similar for all three systems $InNbO_4$, $MnNb_2O_6$, and $YNbO_4$. Interestingly, the major component was not the expected benzyl alcohol but dibenzyl ether, which is rather unusual for this type of nonaqueous sol–gel synthesis. Clearly, one of the intermediates is acting as a dehydration/etherification catalyst. Furthermore, the mixture also contained substantial amounts of benzyl alcohol, benzyl acetate, and 2-benzylbenzyl alcohol, as well as minor quantities of 3-benzylbenzyl alcohol, acetone, benzaldehyde, diphenylmethane, 4-benzyltoluene, 4-phenyl-3-buten-2-one, and traces of several other polyaromatic compounds, including 1,4-bisbenzylphenol, stilbene, 3,3′-dimethylbiphenyl, and 1,2,3,4-tetraphenylbutane.

We recently studied the reaction of several metal acetylacetonates, including $In(acac)_3$, in benzylamine, which led to the formation of In_2O_3 nanocrystals under conditions similar to those used herein.[23] The oxide formation commenced with a solvolysis of the acetylacetonate ligands to result in *N*-benzylacetamide and enolate ligands, which underwent ketimine-type condensation reactions in the second step to form imines and metal-coordinated hydroxy groups that induced the oxide formation. We also investigated the reaction of $Fe(acac)_3$ in benzyl alcohol, and it was found to involve a similar reaction sequence. First, benzyl alcohol induces solvolysis of the acetylacetonate to benzyl acetate and acetone (which remains bound to the metal center as an enolate ligand). Then, an addition reaction of the enolate ligand and benzyl alcohol, catalyzed by the metal center, takes place, which results in metal-coordinated hydroxy groups that induce further condensation to the oxide, as well as 4-phenyl-2-butanone as a side product.[24]

In the systems investigated herein, the acetylacetonate ligands also undergo a metal-promoted, effective alcoholysis, as shown by the formation of acetone and benzyl acetate as well as the absence of any acetylacetone signals in the NMR spectra (Scheme 2a). Interestingly, further condensation of

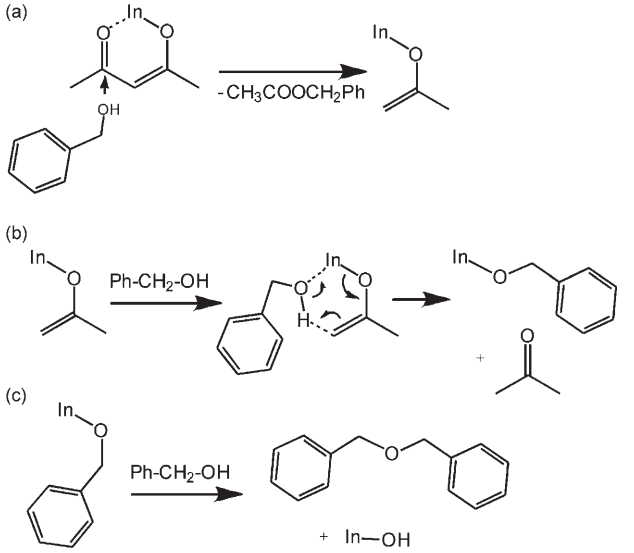

Scheme 2. Main reaction pathway for the formation of the hydroxy species upon reaction of $In(acac)_3$ with benzyl alcohol. a) Solvolysis of acetylacetonate species. b) Ligand-exchange reaction. c) Mechanism of ether condensation.

the enolate species only occurred to a small extent, as the only potential condensation product found in the reaction mixture was 4-phenyl-3-buten-2-one (molar ratio to acetone $\approx$1:4). However, the main reaction enabling oxide formation proceeded by a ligand-exchange reaction to release acetone through coordination of benzyl alcohol to the Nb metal center (Scheme 2b) followed by ether elimination (Scheme 2c). The catalyzed ether-formation reaction proceeded to a very large extent, thus resulting not only in hydroxy species that induced the formation of $In(OH)_3$, but also in free water that separated from the organic medium.

Notably, this ether formation took place only in the presence of $NbCl_5$ in the system, as no ethers were formed upon the reaction of acetylacetonates with benzyl alcohol. Interestingly, no benzyl chloride or other alkyl halides formed during the reaction, thus indicating the strong preference of ether formation over alkyl halide elimination. These observations were previously reported by Li and co-workers[25] and also in the synthesis of TiO_2 in benzyl alcohol with various organic ligands.[24] Therefore, the only remaining question is the fate of the chloride ligands of $NbCl_5$. As the Nb center evidently acts as catalyst for ether formation, the water produced would hydrolyze the chloride to form metal-bound hydroxy groups. We propose that the chloride then forms hydrochloric acid (a weaker acid than $NbCl_5$), a

CHEMISTRY
AN ASIAN JOURNAL

hypothesis supported by the high acidity (pH 1) of the aqueous phase. The presence of chloride ions in the aqueous phase was proven by the silver nitrate test. The large number of additionally formed bi- and multiaromatic compounds is attributed to the presence of Nb metal centers in the system, which are known to function as good catalysts for benzylation reactions.[26] In fact, we have already observed such benzylation reactions during the synthesis of $NaNbO_3$ nanocrystals from niobium(V) ethoxide in benzyl alcohol.[24] Still, it is notable that these benzylations also proceed in the presence of a second, aqueous phase in the system.

In summary, three processes were identified to occur almost simultaneously during particle formation. Whereas the Nb-mediated condensation of benzyl alcohol to benzyl ether supplies water for the formation of hydroxide species, amorphous intermediates, and finally particle formation, the acetylacetonate ligands undergo solvolysis. Owing to the high-temperature conditions in the system, additionally occurring benzylation reactions lead to the formation of multiaromatic compounds as side products. Notably, in the $YNbO_4$ sample, the formal water required for oxide formation is in principle already present in the used precursor. Thus, no further elimination of water is required, but the ether-condensation reaction still proceeds almost to completion. For the $MnNb_2O_5$ sample, significantly larger amounts of benzaldehyde were found in the final mixture, which explains the formation of Mn^{II} from the manganese(III) precursor. Benzyl chloride was also detected in this sample (see Supporting Information).

Conclusions

We have demonstrated a general approach to the synthesis of transition-metal niobate nanocrystals, such as $InNbO_4$, $MnNb_2O_6$, and $YNbO_4$, by using the one-pot solvothermal reaction of niobium chloride with transition-metal acetylacetonates in benzyl alcohol. The mechanism of formation of these transition-metal niobates is interesting with respect to the crystallization pathway as well as from an organic-chemical point of view. On the one hand, particle formation involves a dissolution–recrystallization process of the crystalline metal hydroxide and amorphous niobium oxide formed in situ as intermediates; on the other, the chemical mechanisms responsible for the oxygen supply are based on three almost-simultaneously occurring processes: 1) benzyl ether elimination as the main pathway mediated by the niobium species, which provides water that is formally required for oxide formation; 2) solvolysis of the acetylacetonate ligand to acetone and benzyl acetate; and 3) benzylation. Instead of alkyl halide elimination, the chlorides turn into HCl, which dissolves in the aqueous phase.

The soft-chemistry synthesis of the metal niobate nanoparticles represents, in our opinion, a relevant step forward in the controlled preparation of complex nanomaterials that are of high scientific and technological relevance.

Experimental Section

Materials

Manganese acetylacetonate (STREM, 97+%), yttrium acetylacetonate hydrate (Aldrich, 99.99%), indium acetylacetonate (Aldrich, 99.99%), niobium chloride (Aldrich, 99.9+%), and anhydrous benzyl alcohol (Aldrich, 99.8+%) were used as precursor materials. Solvothermal treatment was performed in Parr acid digestion bombs with teflon cups (45 mL). As a first step, niobium chloride was ground into a fine powder and stored in a vessel with a punched cap until its color changed completely from yellow to white.

Synthesis

Typically, indium acetylacetonate (1 mmol) or manganese acetylacetonate (0.5 mmol) and niobium chloride (1 mmol) were added to anhydrous benzyl alcohol (20 mL) in a teflon cup. The mixture was then placed in a steel autoclave and heated in a furnace at 200 °C for 1–4 days. Upon cooling to room temperature, the resulting precipitate was collected by centrifugation, washed thoroughly with acetone and ethanol, and dried at 60 °C in air.

Characterization

XRD patterns of all samples were gathered in reflection mode ($Cu_{K\alpha}$ radiation) on a Bruker D8 diffractometer equipped with a scintillation counter. TEM was performed on a Zeiss EM 912Ω instrument at an acceleration voltage of 120 kV. HRTEM and EDX were performed with a Philips CM200-FEG microscope (200 kV, $C_s = 1.35$ mm). Nitrogen-adsorption and -desorption isotherms were obtained at 77 K with a Micrometritics ASAP2010 system after the samples were vacuum-dried at 160 °C overnight. The reaction mechanisms were investigated by retro-analysis by using reaction solutions obtained after the removal of particulate products by centrifugation and filtration. The initial concentration of the precursor species was increased by decreasing the amount of benzyl alcohol to 5 mL to obtain well-detectable amounts of organic by-products. GC–MS analysis was carried out on a GC 6890 N device (Agilent Technologies). The liquids were directly injected into the GC device. ^{1}H-decoupled ^{13}C NMR spectroscopy was performed on a Bruker DPX 400 spectrometer at 100 MHz on samples diluted with $CDCl_3$ at a sample spinning rate of 20 Hz and with the ZG30 pulse program.

Acknowledgements

We thank Dr. Frederic Goettmann for performing the GC–MS. Financial support by the Max-Planck-Society is gratefully acknowledged. L.Z. is grateful for financial support from the Alexander von Humboldt Foundation, the National Basic Research Program of China (973 Program) (Grant 2007CB613301), and the National Science Foundation of China (Grants 20503009 and 20777026).

[1] Y. B. Mao, T. J. Park, S. S. Wong, *Chem. Commun.* **2005**, 5721.
[2] M. Valant, A. K. Axelsson, N. Alford, *Chem. Mater.* **2007**, *19*, 5431.
[3] L. Xu, Y. Su, Q. Zhou, S. Li, Y. Chen, Y. Feng, *Cryst. Growth Des.* **2007**, *7*, 810.
[4] J. Chen, X. R. Xing, A. Watson, W. Wang, R. B. Yu, J. X. Deng, L. Yan, C. Sun, X. B. Chen, *Chem. Mater.* **2007**, *19*, 3598.
[5] C. W. Yao, Q. S. Zeng, G. F. Goya, T. Torres, J. F. Liu, H. P. Wu, M. Y. Ge, Y. W. Zeng, Y. W. Wang, J. Z. Jiang, *J. Phys. Chem. C* **2007**, *111*, 12274.
[6] S. O'Brien, L. Brus, C. B. Murray, *J. Am. Chem. Soc.* **2001**, *123*, 12085.
[7] A. E. Henkes, J. C. Bauer, A. K. Sra, R. D. Johnson, R. E. Cable, R. E. Schaak, *Chem. Mater.* **2006**, *18*, 567.
[8] S. H. Sun, H. Zeng, D. B. Robinson, S. Raoux, P. M. Rice, S. X. Wang, G. X. Li, *J. Am. Chem. Soc.* **2004**, *126*, 273.
[9] Q. Song, Z. J. Zhang, *J. Am. Chem. Soc.* **2004**, *126*, 6164.

[10] M. Niederberger, N. Pinna, J. Polleux, M. Antonietti, *Angew. Chem.* **2004**, *116*, 2320; *Angew. Chem. Int. Ed.* **2004**, *43*, 2270.
[11] M. Niederberger, G. Garnweitner, N. Pinna, M. Antonietti, *J. Am. Chem. Soc.* **2004**, *126*, 9120.
[12] G. Garnweitner, J. Hentschel, M. Antonietti, N. Niederberger, *Chem. Mater.* **2005**, *17*, 4594.
[13] G. Garnweitner, M. Niederberger, *J. Am. Ceram. Soc.* **2006**, *89*, 1801.
[14] J. H. Ba, D. Fattakhova-Rohlfing, A. Feldhoff, T. Brezesinski, I. Djerdj, M. Wark, M. Niederberger, *Chem. Mater.* **2006**, *18*, 2848.
[15] L. Zhang, I. Djerdj, M. Cao, M. Antonietti, M. Niederberger, *Adv. Mater.* **2007**, *19*, 2083.
[16] M. Niederberger, H. Colfen, *Phys. Chem. Chem. Phys.* **2006**, *8*, 3271.
[17] J. H. Ba, A. Feldhoff, D. Fattakhova-Rohlfing, M. Wark, M. Antonietti, M. Niederberger, *Small* **2007**, *3*, 310.
[18] Z. B. Wu, N. Kumagai, M. Yoshimura, *Chem. Mater.* **2000**, *12*, 3356.
[19] J. C. Yu, L. Z. Zhang, Q. Li, K. W. Kwong, A. W. Xu, J. Lin, *Langmuir* **2003**, *19*, 7673.
[20] J. O. Eckert, Jr., C. C. Hung-Houston, B. L. Gersten, M. M. Lencka, R. E. Riman, *J. Am. Ceram. Soc.* **1996**, *79*, 2929.
[21] P. Pinceloup, C. Courtois, A. Leriche, B. Thierry, *J. Eur. Ceram. Soc.* **1999**, *19*, 973.
[22] R. I. Walton, F. Millange, R. I. Smith, T. C. Hansen, D. O'Hare, *J. Am. Chem. Soc.* **2001**, *123*, 12547.
[23] N. Pinna, G. Garnweitner, M. Antonietti, M. Niederberger, *J. Am. Chem. Soc.* **2005**, *127*, 5608.
[24] M. Niederberger, G. Garnweitner, *Chem. Eur. J.* **2006**, *12*, 7282.
[25] C. Wang, Z. X. Deng, G. H. Zhang, S. S. Fan, Y. D. Li, *Powder Technol.* **2002**, *125*, 39.
[26] Y. Rao, M. Trudeau, D. Antonelli, *J. Am. Chem. Soc.* **2006**, *128*, 13996.

Received: September 24, 2007
Published online: March 11, 2008

